Selective *In Vivo* and *In Vitro* Effects of a Small Molecule Inhibitor of Cyclin-Dependent Kinase 4

Rajeev Soni, Terence O'Reilly, Pascal Furet, Lionel Muller, Christine Stephan, Sabine Zumstein-Mecker, Heinz Fretz, Doriano Fabbro, Bhabatosh Chaudhuri

Background: **Cyclin-dependent kinase 4 (Cdk4) represents a prime target for the treatment of cancer because most human cancers are characterized by overexpression of its activating partner cyclin D1, loss of the natural Cdk4-specific inhibitor p16, or mutation(s) in Cdk4's catalytic subunit. All of these can cause deregulated cell growth, resulting in tumor formation. We sought to identify a small molecule that could inhibit the kinase activity of Cdk4 *in vitro* and to then ascertain the effects of that inhibitor on cell growth and tumor volume *in vivo*. *Methods:* A triaminopyrimidine derivative, CINK4 (a chemical inhibitor of Cdk4), was identified by screening for compounds that could inhibit Cdk4 enzyme activity *in vitro*. Kinase assays were performed on diverse human Cdks and on other kinases that were expressed in and purified from insect cells to determine the specificity of CINK4. Cell cycle effects of CINK4 on tumor and normal cells were studied by flow cytometry, and changes in phosphorylation of the retinoblastoma protein (pRb), a substrate of Cdk4, were determined by western blotting. The effect of the inhibitor on tumor growth *in vivo* was studied by use of tumors established through xenografts of HCT116 colon carcinoma cells in mice. Statistical tests were two-sided. *Results:* CINK4 specifically inhibited Cdk4/cyclin D1 *in vitro*. It caused growth arrest in tumor cells and in normal cells and prevented pRb phosphorylation. CINK4 treatment resulted in statistically significantly ($P = .031$) smaller mean tumor volumes in a mouse xenograft model. *Conclusions:* Like p16, the natural inhibitor of Cdk4, CINK4 inhibits Cdk4 activity *in vitro* and slows tumor growth *in vivo*. The specificity of CINK4 for Cdk4 raises the possibility that this small molecule or one with a similar structure could have therapeutic value. [J Natl Cancer Inst 2001;93: 436–46]**

Progression through the cell cycle is regulated by the activity of various cyclin-dependent kinases, their cyclin partners, and cognate inhibitor proteins *(1–6).* Cyclin-dependent kinase 4 (Cdk4) is an important cell cycle kinase, since its activity is required for initiating the phosphorylation of the retinoblastoma protein (pRb). This triggers a cascade of events that compels cells toward an irreversible commitment to proliferation *(7–9).* In its hypophosphorylated form, pRb sequesters the E2F family of transcription factors *(10),* which prevent cells from initiating DNA synthesis. Hyperphosphorylation of pRb, which is initiated by Cdk4 and completed by Cdk2 and Cdk6, releases the sequestered transcription factors, resulting in the loss of pRb's growth-inhibitory function *(8),* thus allowing cells to enter S phase.

The activity of Cdk4 is negatively regulated by $p16^{INK4A}$, hereafter referred to as p16, which acts by binding to Cdk4 and preventing its association with cyclin D1 as well as the subsequent phosphorylation of pRb *(6,11,12).* p16 can thus be thought of as preventing aberrant activation of Cdk4 under normal conditions. When functional p16 is absent because of mutation, deletion, or transcriptional silencing of the gene, cells undergo unregulated proliferation that results in tumor formation *(13,14).* Conversely, ectopic overexpression of p16 causes cells to arrest in G_1. This p16-mediated arrest is dependent on the presence of functional pRb *(11,15–17).* It has been observed that there is a natural inverse relationship between the presence of p16 and pRb in more than 60% of human cancers *(18,19).* In tumors deficient in p16, pRb is always present in an intact and functional form. Unmutated p16 is usually present in tumors that lack functional pRb. Moreover, the majority of human cancers have

Affiliations of authors: R. Soni, T. O'Reilly, P. Furet, L. Muller, C. Stephan, S. Zumstein-Mecker, H. Fretz, D. Fabbro, Oncology Research, Novartis Pharma AG, Basel, Switzerland; B. Chaudhuri, Leicester School of Pharmacy, De Montfort University, U.K.

Correspondence to: Professor Bhabatosh Chaudhuri, Leicester School of Pharmacy, De Montfort University, The Gateway, Leicester LE1 9BH, U.K. (bchaudhuri@dmu.ac.uk).

See "Notes" following "References."

either constitutively activating mutations in Cdk4 that prevent p16-mediated Cdk4 inhibition or inactivating mutations in p16 itself or they overexpress the Cdk4-activating partner cyclin D1 and/or have lost active pRb *(5).* These findings imply that deregulation of Cdk4 activity can cause the unrestricted cell growth that results in tumor formation.

The link between Cdk4 activation and pRb phosphorylation and the crucial role that this pathway plays in cell cycle progression makes Cdk4 an important therapeutic target in cancer. It is conceivable that inhibition of Cdk4 would prevent unregulated growth of cancer cells. That is, a Cdk4-specific inhibitor in a p16-deficient, pRb-positive cell would prevent Cdk4 from phosphorylating pRb, which would lead to a G_1 block in the cell cycle and thereby prevent cell proliferation. Like p16, the inhibitor would have no effect on pRb-deficient cells or on cells that contain inactivated pRb.

Using a recently described screen that identifies novel small molecule inhibitors of Cdk4 activity *(20),* we identified CINK4 (a chemical inhibitor of Cdk4) as a compound that specifically inhibits Cdk4 in an *in vitro* enzyme assay. We have now tested the efficacy of CINK4 as an inhibitor of cell growth *in vitro* by treating tumor cell lines and *in vivo* by using an established mouse tumor model.

Materials and Methods

Identification of CINK4

A high throughput screen was used to monitor the *in vitro* phosphorylation of pRb by human recombinant Cdk4/cyclin D1 enzyme purified from insect cells in the presence or absence of compounds from a library of potential small molecule inhibitors of Cdk4 *(20).* CINK4 is one such compound that inhibited pRb phosphorylation in this screen.

Chemistry

CINK4 was prepared in a three-step synthesis starting with 2,4,6-trichloropyrimidine. All starting materials were obtained from Fluka (Buchs, Switzerland). First, *trans*-4-amino-cyclohexanol (20.8 mL [0.15 mol]) was reacted in an ethanol solution (90 mL) with 2,4,6-trichloropyrimidine (17.17 mL [0.15 mol]) in the presence of triethylamine (20.8 mL [0.15 mol]) at room temperature for 5 hours to give a mixture of the 2- and 4-substituted regioisomers of 4-(2,6-dichloro-pyrimidin-4-ylamino)-cyclohexanol. After chromatographic separation on silica gel, 4-(2,6-dichloro-pyrimidin-4-ylamino)-cyclohexanol (11.8 g [0.045 mol]) was treated with 1-benzyl-1*H*-indol-5-ylamine (8.9 g [0.04 mol]) and triethylamine (10 mL [0.072 mol]) in ethanol at 150 °C for 24 hours. The resulting compound, 4-(2-[1-benzyl-1*H*-indol-5-ylamino]-6-chloro-pyrimidin-4-ylamino)-cyclohexanol (7.0 g [0.016 mol]) was heated with aqueous ethylamine (100 mL, 70% [1.25 mol]) in a sealed tube at 130 °C for 24 hours, yielding yellowish crystals of CINK4 (melting point, 204 °C–205 °C). The integrity and purity of the final compound and the intermediates were assessed by nuclear magnetic resonance (NMR) spectroscopy (^{1}H-, ^{13}C NMR, nuclear Overhauser effect) and mass spectrometric and combustion analyses. By these criteria, the CINK4 used in this study was 100% pure.

Kinase Assays

The human cyclins A, B, E, D1, and D2 were co-expressed as glutathione *S*-transferase (GST) fusion proteins in Sf9 insect cells with the Cdk catalytic subunits (Cdks 1, 2, 4, and 6) as described previously *(21–24).* The holoenzymes, containing a Cdk bound to a GST cyclin, were purified by use of reduced glutathione (GSH)–Sepharose (Amersham-Pharmacia, Zurich, Switzerland). The human tyrosine kinases v-abl, c-met, IGF-1R, and Insulin-R were also expressed as GST fusions in Sf9 cells and were purified over GSH–Sepharose exactly like the Cdk holoenzymes. Kinase reactions were performed as described previously *(20,25–27)* by use of purified tyrosine kinases or the recombinant cyclins complexed with Cdk catalytic subunits in a 1 : 1 ratio in the presence and in the absence of CINK4 by use of the radioactive label [^{33}P]adenosine triphosphate (ATP). GST-pRb(152) (Santa-Cruz Biotechnology, Santa Cruz, CA), which contains the C-terminal 152 amino acid fragment of pRb, was used as a substrate for all Cdk enzyme assays, whereas routinely used protein tyrosine kinase peptide substrates that contain a unique tyrosine residue were used for the specific tyrosine kinase assays *(24–27).* Kinase activity was detected and/or measured by phosphorimage quantitation. All kinase assays were performed in duplicate and represent an average of three independent experiments. Using 10 empirically determined concentrations between 0 and 100 μ*M* of CINK4, we determined the concentration of CINK4 that inhibited 50% of the activity of each kinase (IC_{50}). The IC_{50} was obtained by plotting the percentage of total radioactive counts incorporated into the substrate by a kinase at a certain concentration of inhibitor compared with total counts incorporated in the absence of CINK4 versus the concentration of the inhibitor.

Interactive Modeling Studies

The modeling work was performed by use of MacroModel version 4.0 software *(28)* to verify our observations in secondary *in vitro* enzyme assays that CINK4 inhibits Cdk4 but not Cdk2. Our Cdk4 model is based on the published coordinates of a Cdk2–ATP complex *(29)* that keeps the Cdk2 amino acid residues within 6 &ARING; of any atom of ATP. We used the sequence alignments reported by Hanks and Quinn *(30)* to identify the amino acid residues that differed between Cdk4 and Cdk2. Those residues in Cdk2 (Phe 82, Leu 83, His 84, Lys 89, and Gln 131) were then changed in the model to the analogous residues in Cdk4 (His 95, Val 96, Asp 97, Thr 102, and Glu 144, respectively), so that similar rotameric states for the amino acid side chains were maintained.

Interactive docking experiments were performed after ATP was removed from the model and replaced with the structure of CINK4 to determine whether CINK4 could compete with ATP for binding to Cdk4. The orientations of CINK4 and Cdk4 shown in Fig. 1 were considered to be satisfactory because of the strict overlap of the Cdk4/ATP and Cdk4/CINK4 coordinates. The resulting model was energy minimized to find the best nearby conformation [using modified Assisted Model Building With Energy Refinement (AMBER*) software (http://www.amber.ucsf.edu/amber/amber.html) force field with the GB/SA solvation model *(31,32)*] by keeping the amino acids within the ATP-binding site of Cdk4 rigid.

Cell Culture

All cells were cultured at 37 °C in 5% CO_2 in medium supplemented with 10% fetal calf serum and 1% penicillin/streptomycin (both from Life Technologies, Inc. [GIBCO BRL], Rockville, MD). U2OS human osteosarcoma and NIH3T3 mouse fibroblast cells were grown in Dulbecco's modified Eagle medium (DMEM) and high glucose (4500 mg/L) with stable glutamine (AMIMED, Allschwil, Switzerland). MRC-5 human fibroblast cells were grown in DMEM and low glucose (1000 mg/L) with stable glutamine (AMIMED).) HCT116 human colon carcinoma cells were grown in McCoy's 5A medium with stable glutamine (AMIMED). U2OS and HCT116 cells lack p16 and express functional pRb (pRb positive and p16 negative), whereas NIH3T3 and MRC-5 cells express functional pRb and p16 (pRb positive and p16 positive).

Exponentially growing cells, representing an asynchronous population, were seeded at a density of 7.5×10^4 cells/mL in 10 mL of medium per T75 flask and grown for 24 hours before being treated with CINK4. CINK4 was dissolved in 10% dimethyl sulfoxide (DMSO) to make 100× stock solutions and was added to cells at final concentrations of 5 and 10 μ*M*. Cells were then incubated for another 24 hours, after which they were harvested and washed once with phosphate-buffered saline (PBS). For western blotting, the washed cells were then frozen at −80 °C. For flow cytometry analyses, washed cells were fixed in 70% ethanol at −20 °C overnight and kept at −20 °C. For detection of apoptosis, treated cells were harvested, washed with PBS, and fixed with 2% paraformaldehyde for 15 minutes on ice. Cells were washed again with PBS, fixed in 70% ethanol at −20 °C overnight, and stored at −20 °C. All experiments were performed at least twice under similar conditions to ensure reproducibility.

Quinidine and roscovitine were purchased from Sigma Chemical Co. (St. Louis, MO), and 100× stock solutions of each were prepared in 10% DMSO. Cells were treated with quinidine at a concentration of 50 μ*M* for 24 hours to block them in the early G_1 phase of the cell cycle. Serum-starved and mimosine-treated cells were released in the presence of 10 μ*M* roscovitine.

Mimosine (CALBIOCHEM AG, Lucerne, Switzerland) was prepared as a 100× stock solution in 10% DMSO and was added to cells at a final concentration of 0.2 m*M*. Cells were treated for 32 hours with mimosine, after which they were washed and then released into fresh medium lacking mimosine in the presence and absence of CINK4.

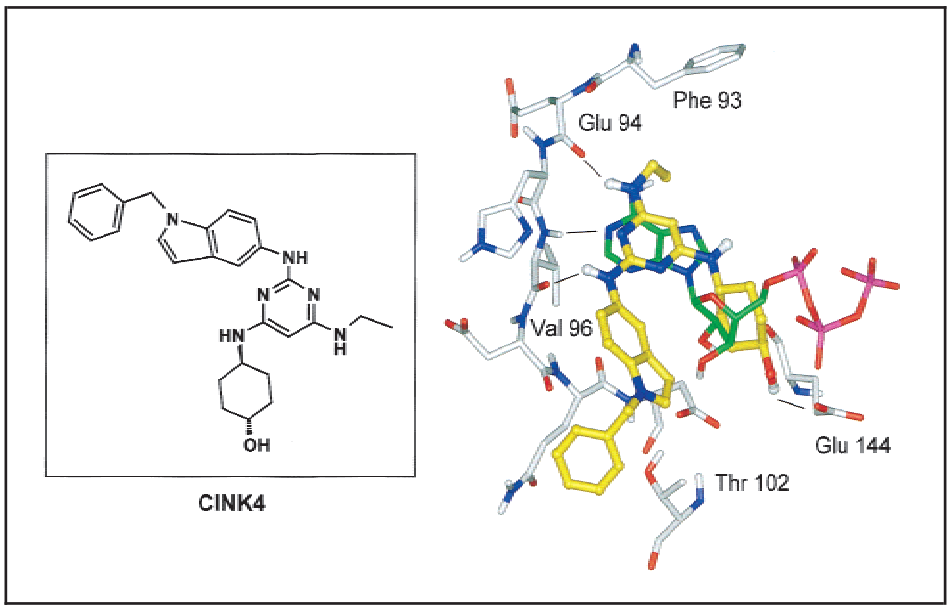

Fig. 1. Structure of CINK4 (a chemical inhibitor of Cdk4) and its predicted mode of binding to Cdk4 (cyclin-dependent kinase 4). Structure and model of the relative binding modes of CINK4 (**yellow**) and adenosine triphosphate (ATP) (**green**) in the ATP pocket of Cdk4 (**gray**). In this model, the structures of CINK4 and ATP are superimposed to facilitate comparison of their interactions with Cdk4. Hydrogen bonds are indicated by **thin black lines.**

MRC-5 and HCT116 cells were serum starved for 72 hours in medium containing 0.1% serum, then released into 10% serum-containing medium with and without 5 and 10 μ*M* CINK4 for 24 hours.

Immunoprecipitation of Cdk4/Cyclin D Complexes

A Cdk4 antibody (product number sc-260; Santa Cruz Biotechnology, Santa Cruz, CA), immobilized on protein A–Sepharose beads, was used to immunoprecipitate Cdk4-bound cyclin D complexes from CINK4-treated HCT116 cells. Lysates were prepared by solubilizing cells in IP buffer (i.e., 25 m*M* Tris–HCl [pH 7.5], 60 m*M* β-glycerophosphate, 15 m*M* $MgCl_2$, 15 m*M* EGTA, 0.1 m*M* sodium fluoride, 15 m*M* *p*-nitrophenyl phosphate, 1 m*M* dithiothreitol, 0.1 m*M* phenylmethylsulfonyl fluoride [PMSF], and 0.1% Nonidet P-40). Immunoprecipitations were carried out in IP buffer by use of equal amounts of total protein (300 μg). The beads were washed eight times with 1 mL of ice-cold IP buffer and 1 mL of ice-cold wash buffer (50 m*M* Tris–HCl [pH 7.5], 10 m*M* $MgCl_2$, and 1 m*M* dithiothreitol) before being used for the *in vitro* Cdk4 kinase assay (using pRb as substrate).

Cell Cycle Analysis

Cells fixed in 70% ethanol were centrifuged for 1 minute at 3000*g* at 25 °C, washed once with PBS, treated with 3 mg/mL ribonuclease (Sigma Chemical Co.) for 30 minutes at 37 °C, and stained with 50 μg/mL propidium iodide (Sigma Chemical Co.) for 1 hour at room temperature. Flow cytometry analyses were performed on the Becton Dickinson fluorescence-activated cell sorter-calibur (Becton Dickinson, Zurich, Switzerland) by use of the Becton Dickinson Cell Quest program. Flow cytometry data were acquired with the use of linear amplification of the fluorescence area measurement (FL-2) and pulse processing (area versus width) to gate on single events, with the total event rate not exceeding 300 events/second. Data acquisition was set to stop after 9 minutes or after a minimum of 10 000 events had been collected in the single-events region.

Apoptosis Detection Assay

The terminal deoxynucleotidyl transferase-mediated bromodeoxyuridine (BrdU) triphosphate nick end-labeling (TUNEL) assay, which detects DNA strand breaks, was performed with the use of the APO-BRDU kit (Phoenix Flow Systems, San Diego, CA) according to manufacturer's instructions to detect apoptosis. Apoptosis was quantified by use of flow cytometry. We also used the Cell Death Detection Enzyme-Linked Immunosorbent Assay kit (Roche Molecular Diagnostics, Basel, Switzerland), according to the manufacturer's instructions to detect DNA fragmentation.

Western Blot Analyses

The frozen cell pellets were thawed and lysed in 100–200 μL of RIPA buffer (i.e., 25 m*M* Tris–HCl [pH 7.5], 1 m*M* EDTA, 50 m*M* NaCl, 0.5% sodium deoxycholate, 0.1% sodium dodecyl sulfate [SDS], 0.1% Tween 20, 50 m*M* β-glycerophosphate, 0.2 m*M* dithiothreitol, 2 m*M* sodium orthovanadate, 1 m*M* PMSF, 10 μg/mL Antipain, 10 μg/mL Leupeptin, and 1× Complete™ Protease inhibitors [Roche Molecular Diagnostics]) at 4 °C. The samples were centrifuged for 15 minutes at 4 °C at 10 000 rpm. Protein concentrations of the resulting supernatants were determined by use of the Bio-Rad Protein Assay (Bio-Rad, Zurich, Switzerland). Equal amounts of protein (20 μg) were separated on 7.5% (for pRb western blots) and 12.5% (for Cdk4, cyclin D1, cdc2, and cyclin A western blots) SDS–polyacrylamide gels and transferred to Immobilon-P Transfer Membrane (Millipore Corp., Zurich, Switzerland). The membranes were probed with the following primary antibodies: Cdk4-Ab (product number sc-260 from Santa Cruz Biotechnology) at 1 : 100 dilution to detect Cdk4; Ab-5 (product number OP-66 from CALBIOCHEM AG) at 1 : 200 dilution to detect phosphorylated and unphosphorylated full-length pRb; C-15 (product number sc-50 from Santa Cruz Biotechnology) at 1 : 2000 dilution to detect the carboxy-terminal 15 amino acids of pRb; Ser795 (New England Biolabs, Inc., Basel, Switzerland) at 1 : 200 dilution to detect phosphorylation of pRb at serine residue 795; Ser780 (batch number SZ254 raised at Novartis, Basel, Switzerland) at 1 : 20 dilution to detect phosphorylation of pRb at serine residue 780; and P-Tyr-100 (product number 9411 from New England Biolabs, Inc.) at 1 : 2000 dilution to detect phosphorylation of tyrosine residue 15 in all Cdks. The secondary antibody was horseradish peroxidase-conjugated anti-rabbit immunoglobulin G. Bands were visualized by chemiluminescence by use of the ECL kit (Amersham-Pharmacia, Zurich, Switzerland).

Detection of Senescence-Associated β-Galactosidase

After 24 hours of treatment with CINK4, cells were washed with PBS, fixed in 0.5% glutaraldehyde solution in water for 2 minutes, washed again in PBS, and stained with X-gal solution (i.e., 1 mg/mL X-gal, 0.12 m*M* $K_3Fe[CN]_6$, 0.12 m*M* $K_4Fe[CN]_6$, and 1 m*M* $MgCl_2$ in PBS [pH 6.0]) overnight at 37 °C. Photographs were taken after an overnight incubation at 37 °C with the staining solution. All reagents were purchased from Sigma Chemical Co.

In Vivo CINK4 Experiments

The Ethical Committee of the Cantonese Veterinäramt of Basel Stadt approved all experimental protocols involving animals. Female BALB/c nu/nu (nude) mice (19–21 g in body weight) were obtained from Iffa Credo (L'Arbresle, France).

Adherent HCT116 cells were washed once with Hanks' buffer (Life Technologies, Inc.), treated with 0.25% trypsin, washed again with Hanks' buffer, and adjusted to a final concentration of 1×10^7 viable cells/mL in Hanks' buffer based on trypan blue staining. This suspension (0.1 mL) was injected subcutaneously into each of 24 mice (eight mice per treatment group). Twenty days later, when tumors derived from those cells had reached a volume of approximately 100 mm^3, the actual tumor volumes were measured by use of calipers,

and those values were used to estimate tumor volume according to the formula: volume (mm^3) = length (mm) × width (mm^2) × π/6. The mice were then placed into three groups containing eight mice each, the groups were randomly assigned with respect to treatment, and treatment with CINK4, 5-fluorouracil, or control was initiated. CINK4 was administered by intraperitoneal injection at a dose of 30 mg/kg every 12 hours, while 5-fluorouracil (Roche Pharma Schweiz, Reinach, Switzerland) was administered by intravenous injection into a lateral tail vein at a dose of 75 mg/kg once per week. Mice in the control group received the CINK4 diluent (5% DMSO, 0.05% Tween 80, and 95% physiologic saline) by intraperitoneal injection. All treatments were administered at a constant volume (10 mL/kg) for 29 days. Tumor volumes were measured by a blinded procedure at 2–4-day intervals throughout the treatment period. Body weights (in g) were also measured at the same frequency. There was one death, which occurred in the CINK4 treatment group, on the final day of the experiment.

Statistical Methods Used for Analyses of *In Vivo* Results

We determined the efficacy of various *in vivo* treatments by calculating the change in tumor volume over time. Because changes in tumor volumes were not always normally distributed, the data were logarithmically transformed to a normal distribution. One-way analysis of variance (ANOVA) by use of Dunnett's test was used to compare changes in tumor volumes in mice treated with CINK4 or 5-fluorouracil with those in the control animals. The influence of treatment on tumor growth rate was determined by comparing the slopes of a plot of log tumor volume versus time from each mouse by one-way ANOVA by use of the two-sided Student's *t*–Newman–Keuls tests for multiple pairwise comparisons of all groups. The differences between final and initial body weights were compared, by use of two-sided paired Student's *t* tests, to determine that these differences were distributed normally. For all tests, the level of significance was set at $P<.05$. Note that, for these small sample sizes, the desired power level of 0.8 was not always obtained. Statistical calculations were performed by use of SigmaStat 2.03 (Jandel Scientific, San Rafael, CA). Statistical tests were two-sided.

RESULTS

Selective Inhibition by CINK4

We identified CINK4 in a high throughput screen for small molecules that could inhibit the phosphorylation of a pRb substrate by Cdk4 *(20).* CINK4 was prepared subsequently in a three-step synthesis that yielded a product that was 100% pure (*see* the "Materials and Methods" section). To ascertain whether the inhibitory activity of CINK4 was selective for Cdk4, we determined the concentrations of CINK4 at which the activities of five purified Cdks and four purified tyrosine kinases were 50% inhibited (IC_{50}) by performing *in vitro* kinase assays in the presence of increasing concentrations of CINK4 by use of purified peptides as substrates *(26–29).* As shown in Table 1, CINK4 showed approximately fourfold more specificity toward Cdk4/cyclin D1 than toward Cdk6/cyclin D1, as determined by IC_{50}s. Of interest, the concentrations of CINK4 required to inhibit the kinase activities of Cdk4 and Cdk6 when these kinases were complexed with cyclin D2 were at least an order of magnitude greater than those required to inhibit these kinases when they were complexed with cyclin D1. This difference may reflect alterations in the three-dimensional structures of Cdks that could result from the binding of different cyclins *(3).* The kinase activity of Cdk2 complexed with either cyclin A or cyclin E was not inhibited at CINK4 concentrations up to 100 μ*M,* while that of Cdk5 complexed with p35 was inhibited by 25 μ*M* CINK4. In contrast to these results, flavopiridol, another Cdk inhibitor that is in phase III clinical trials, inhibits all Cdks to varying extents *(33).* CINK4 did not substantially inhibit four prototypic tyrosine kinases *(34),* providing further evidence for the specificity of CINK4 for Cdk4 (Table 1).

Table 1. IC_{50}* of CINK4 (a chemical inhibitor of cyclin-dependent kinase 4) on various cyclin-dependent kinases and prototypic tyrosine kinases

Cyclin-dependent kinases and other tyrosine kinases	IC_{50} of CINK4, (μ*M*)
Cdk2/cyclin A	>50
Cdk1/cyclin B	>100
Cdk2/cyclin E	>50
Cdk4/cyclin D1	1.5
Cdk4/cyclin D2	>50
Cdk6/cyclin D1	5.6
Cdk6/cyclin D2	>50
Cdk5/p35	25
v-abl	>10
c-met	>10
IGF-1R	>10
Insulin-R	>10

*IC_{50} = the concentration of CINK4 that causes 50% inhibition of kinase activity.

CINK4 and Molecular Modeling Studies

To confirm our experimental observations about the selectivity of CINK4 for Cdk4, we developed a hypothesis for the binding of CINK4 to Cdk4 that was based on interactive docking experiments that modeled theoretical interactions between CINK4 and Cdk4 *(35).* Because the structure of Cdk4 has not yet been determined, we developed a theoretical model of its structure that was based on the x-ray crystal structure of the homologous enzyme Cdk2. Like ATP, CINK4 interacts with Cdk4 at the ATP-binding pocket through hydrogen bonds with residues Glu 94 and Val 96 within the Cdk4 kinase hinge region (Fig. 1). According to this model, selective binding of CINK4 to Cdk4 may depend on its interactions with two Cdk4 residues, Thr 102 and Glu 144, which do not occur at comparable positions in Cdk2. We assume that the phenyl group of the benzylic moiety of CINK4 contacts Cdk4 through the side chain of Thr 102. A similar contact with Cdk2, which contains a bulkier lysine residue in the analogous position, would presumably be prevented by steric hindrance. We also assume that the hydroxy group of CINK4 donates a hydrogen bond to the carboxylate function of Glu 144 in Cdk4. In contrast, the analogous residue in Cdk2 is a glutamine with a weaker potential to accept hydrogen bonds. Further confirmation of our model for the CINK4–Cdk4 interaction comes from kinetic analysis, which indicates that CINK4 inhibits Cdk4 by competing with ATP for binding (data not shown).

Effects of CINK4 on Asynchronous Cells

Results from the *in vitro* enzyme assays led us to believe that, if CINK4 was a specific inhibitor of Cdk4, then it should block growth of asynchronous cells in the G_1 phase of the cell cycle. We, therefore, tested the effects of CINK4 on two different asynchronously growing cell lines: U2OS cells derived from a human osteosarcoma, which lack p16 (p16 negative), and normal human fibroblast-derived MRC-5 cells, which express p16 (p16 positive). U2OS and MRC-5 cells, which both express functional pRb (pRb positive), were treated with 5 and 10 μ*M* CINK4 for 24 hours. These concentrations of CINK4 were used because the concentrations of CINK4 that caused 50% inhibition of growth of a large panel of cell lines were between 5 and 10 μ*M* (Soni R, Chaudhuri B: unpublished data). Flow cytometry analyses of cells treated with CINK4 showed that both U2OS and MRC-5 cells arrest in G_1 of the cell cycle, as shown by an

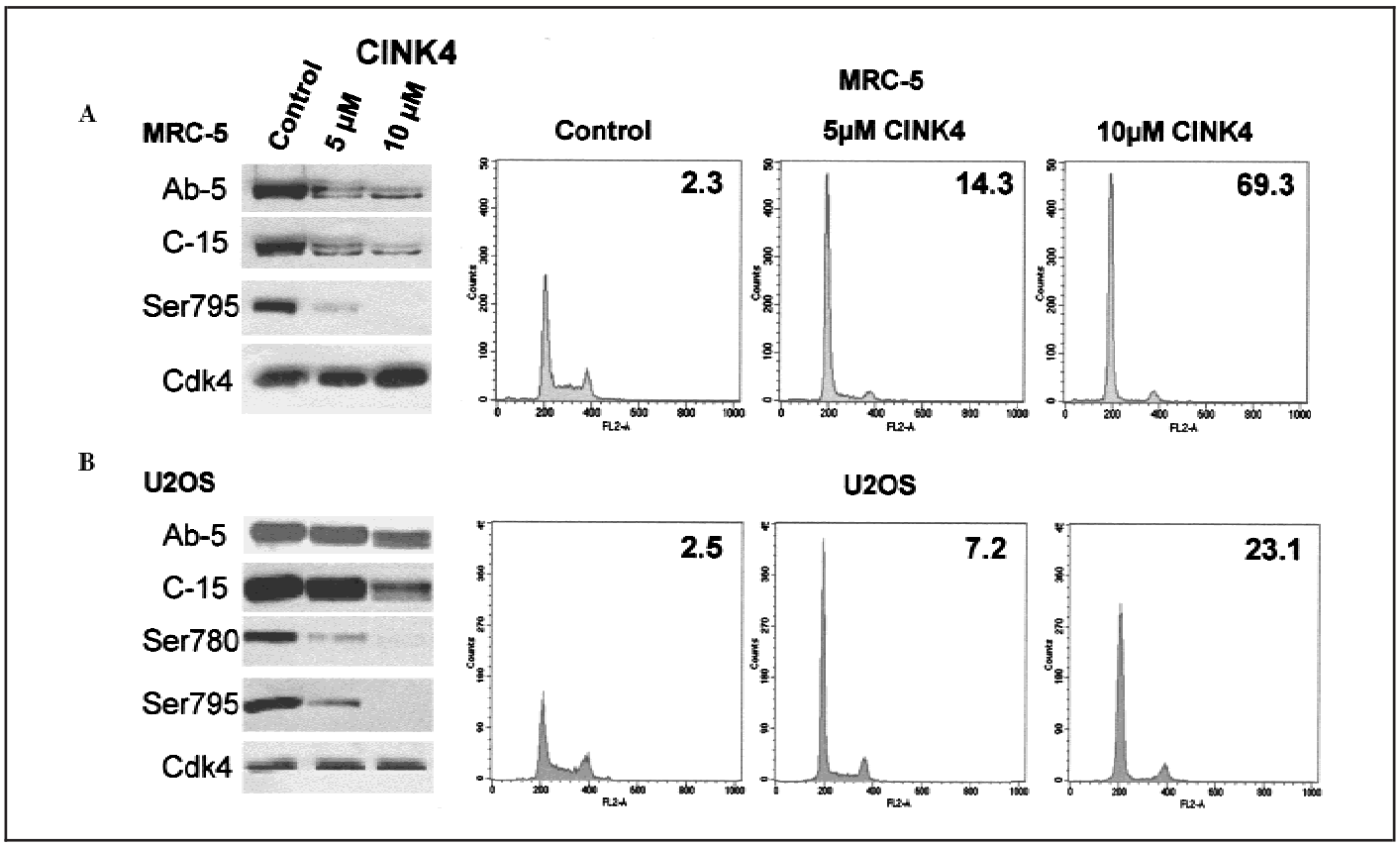

Fig. 2. Western blot and cell cycle analyses of asynchronous MRC-5 (**top**) and U2OS cells (**bottom**) untreated (Control) and treated with 5 and 10 μ*M* CINK4 (a chemical inhibitor of cyclin-dependent kinase 4) for 24 hours. The western blots in **A** and **B,** which were performed on the same cells that underwent cell cycle analysis, were probed with antibodies to detect full-length phosphorylated and unphosphorylated retinoblastoma protein (pRb) (Ab-5), full-length and N-terminally truncated phosphorylated and unphosphorylated pRb (C-15), phosphorylation of pRb at serine residue 780 (Ser780), phosphorylation of pRb at serine residue 795 (Ser795), and the catalytic subunit of the Cdk4 (Cdk4). In each histogram, the ***y*-axis** corresponds to the cell number and the ***x*-axis** refers to the FL-2 area. The cells in G_0/G_1 are represented by a peak at 200 on the *x*-axis, the cells in G_2 are represented by a peak at approximately 400, and the area between those two peaks represents cells in S phase. The number in the **upper right corner** of each histogram represents the ratio of cells in G_1 phase to cells in S phase (G_1/S ratio). A twofold (or greater) difference in G_1/S ratios between the untreated and CINK4-treated cells is taken as evidence of a G_1 arrest *(66).*

increase in the G_0–G_1/S ratio (Fig. 2). However, the block at G_1 was more profound in MRC-5 cells, which express the natural inhibitor of Cdk4, p16. A similar G_1 block was observed in CINK4-treated HCT116 cells (p16 negative and pRb positive; data not shown). The Cdk4 enzyme was immunoprecipitated from CINK4-treated (5 and 10 μ*M*) HCT116 cells and its kinase activity, as monitored by levels of pRb phosphorylation, were substantially less than the kinase activity of Cdk4 enzyme immunoprecipitated from untreated cells (data not shown).

We also analyzed the effect of CINK4 treatment on phosphorylation of endogenous pRb, which is a natural substrate of Cdk4. Treatment of U2OS and MRC-5 cells with 5 and 10 μ*M* CINK4 reduced hyperphosphorylation of pRb, thereby presumably maintaining pRb in an active state (Fig. 2; western blot panels Ab-5 and C-15). CINK4 treatment also caused these cells to incorporate less BrdU into their DNA (data not shown). This result further suggested that pRb in the CINK4-treated cells had undergone a reduction in hyperphosphorylation, because hyperphosphorylation of pRb is necessary for cells to enter S phase and BrdU can be incorporated only when new DNA is synthesized in S phase. Treatment of U2OS and MRC-5 cells with CINK4 also reduced phosphorylation of pRb at serine residues 780 and 795, two sites that are specifically phosphorylated by Cdk4 *(23,36,37)* (Fig. 2). We observed no changes in the levels of Cdk4 in cells that were treated with either concentration of CINK4 (Fig. 2). CINK4 treatment of the human colon carcinoma cell line HCT116, which is p16 negative and pRb positive, gave similar results (data not shown). These observations suggest that CINK4 could function as an inhibitor of Cdk4 in these cells.

Effects of CINK4 Following Serum Starvation and Quinidine Block

Cdk4 is thought to be the first cyclin-dependent kinase that is activated at the G_1/S transition. Cdk4 activation initiates phosphorylation of pRb, which leads to a cascade of events that result in the inactivation of pRb and entry of cells into S phase. The transition from G_0 (quiescence) to the G_1 phase of the cell cycle is dependent on serum growth factors: When cells undergo serum starvation, they arrest at the G_0/G_1 boundary. When fresh serum is added to such cells, they re-enter the cell cycle. We hypothesized that, if CINK4 inhibits Cdk4 *in vivo,* serum-starved cells should not re-enter the cell cycle when they are exposed to fresh medium containing serum and CINK4. Flow cytometric analyses showed that serum-deprived HCT116 (p16 negative and pRb positive) and MRC-5 (p16 positive and pRb positive) cells remained arrested at G_0 or G_1 after they were released into serum-containing medium containing 5 or 10 μ*M*

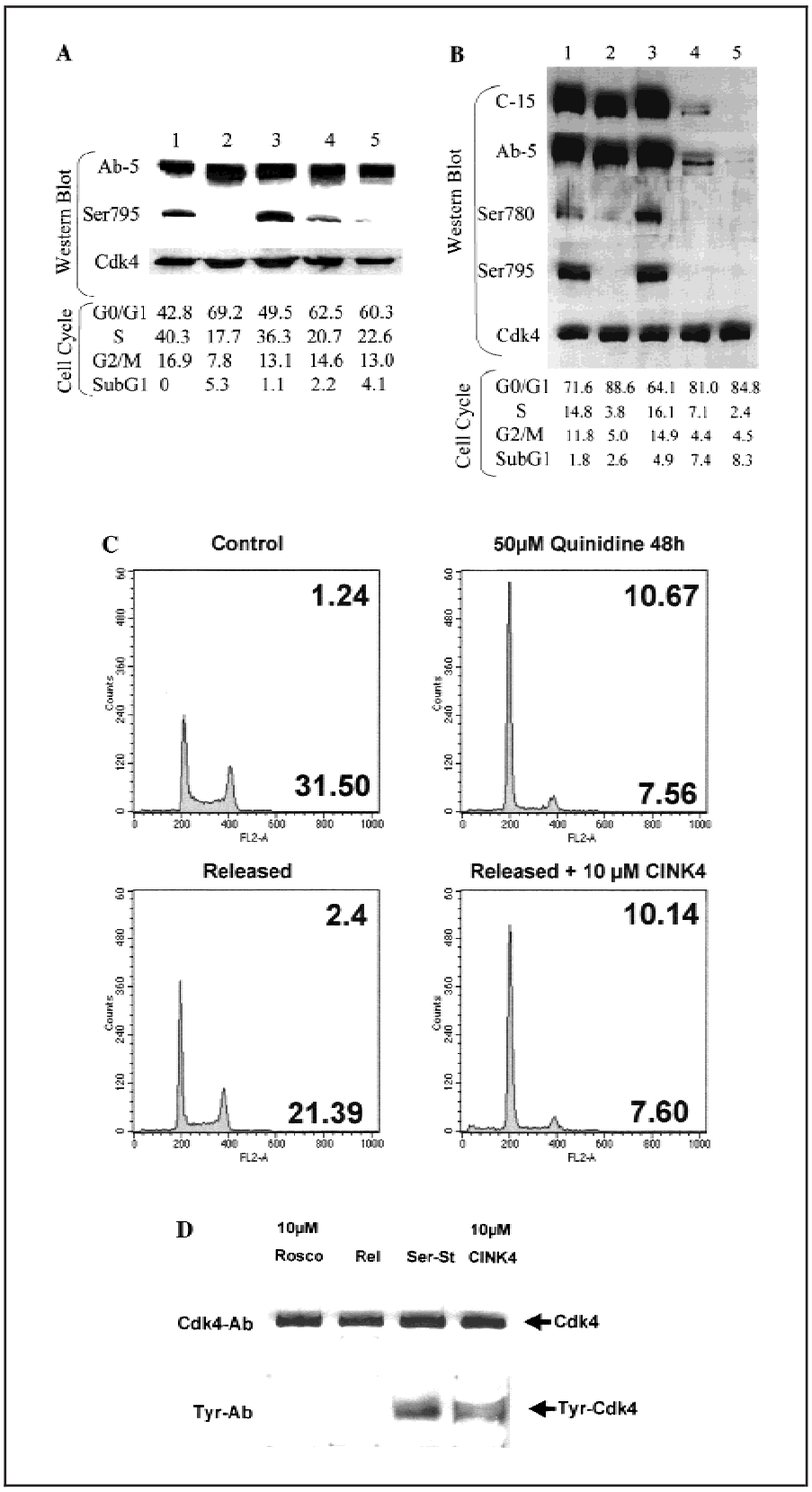

Fig. 3. Effect of CINK4 (a chemical inhibitor of Cdk4) on cell cycle progression and Cdk4 (cyclin-dependent kinase 4) tyrosine phosphorylation. Western blot and cell cycle analyses of serum-starved HCT116 (**A**) and MRC-5 (**B**) cells. The cells were untreated (**lane 1**) or cultured for 72 hours in medium containing 0.1% serum (**lane 2**), then were transferred to medium containing 10% serum without (**lane 3**) or with 5 μ*M* CINK4 (**lane 4**) and 10 μ*M* CINK4 (**lane 5**) for 24 hours. The percentage of cells in G_0/G_1, S, and G_2/M phases, determined by flow cytometry, are shown in the lower half of each figure (Cell Cycle). The western blots, which were performed on the same cells that underwent cell cycle analysis, were probed with antibodies to detect full-length phosphorylated and unphosphorylated retinoblastoma protein (pRb) (Ab-5), full-length and N-terminally truncated phosphorylated and unphosphorylated pRb (C-15), phosphorylation of pRb at serine residue 780 (Ser780), phosphorylation of pRb at serine residue 795 (Ser795), and the catalytic subunit of the Cdk4 (Cdk4). **C**) Cell cycle analysis of U2OS cells. Cells were untreated (Control) or treated with 50 μ*M* quinidine for 48 hours in medium containing 10% serum (50 μ*M* quinidine 48 hours), then were transferred to medium containing 10% serum without (Released) or with (Released + 10 μ*M* CINK4) 10 μ*M* CINK4 for 24 hours. In all histograms, the ***y*-axis** corresponds to the cell number and the ***x*-axis** refers to the FL-2 area. The cells in G_0/G_1 are represented by a peak at 200 on the *x*-axis, the cells in G_2 are represented by a peak at approximately 400, and the area between those two peaks represents cells in S phase. The number in the **upper right corner** refers to the G_1/S ratio, while the number in the **lower corner** refers to the percentage of cells in S phase. Cells released from the quinidine block in the presence of 10 μ*M* CINK4 do not enter the cell cycle. **D**) Western blot analyses of Cdk4 that was immunoprecipitated from HCT116 cells, which were serum starved for 72 hours (Ser-St) in medium containing 0.1% serum and then released into medium containing 10% serum without (Rel) and with 10 μ*M* roscovitine (Rosco) *(45)* or 10 μ*M* CINK4 for 24 hours. Western blots were probed with the same Cdk4 antibody (Cdk4-Ab) used for immunopreciptation and with an antibody (P-Tyr-100) that recognizes phosphorylated tyrosine on proteins.

CINK4 (Fig. 3, A and B). Western blot analyses showed that treatment of the serum-deprived cells with CINK4 also inhibited the phosphorylation of pRb at serine residues 780 and 795 that normally occurs when serum-deprived cells are returned to serum-containing medium (Fig. 3, A and B). Because Cdk4 has been implicated as the kinase that specifically phosphorylates these sites, these results provide further support that CINK4 acts as a specific inhibitor of Cdk4 in these cells *(23,36,37).*

To further confirm that CINK4 prevents cells that are blocked in early G_1 from re-entering the cell cycle, we treated U2OS

cells with the potassium/sodium channel blocker quinidine for 24 hours to inhibit cell growth *(38)* and asked if CINK4 would prevent these cells from entering the cell cycle when they were released into fresh media lacking quinidine. Flow cytometry analyses showed that U2OS cells that were released from a quinidine block into medium containing 10 μ*M* CINK4 failed to enter S phase, while cells released into medium lacking CINK4 did enter S phase (Fig. 3, C). Together, these cell culture results support the hypothesis that CINK4 may act by inhibiting the activity of Cdk4.

Effects of CINK4 on Cdk4 Tyrosine Phosphorylation

Dephosphorylation of tyrosine residue 15 in all Cdks activates these enzymes, and, in the specific case of Cdk4, allows cells to progress through the cell division cycle. Conversely, phosphorylation of this tyrosine residue in Cdk4 prevents serum-starved, quiescent cells from re-entering the cell cycle, and the presence of this phosphorylation is also required for G_1 arrest induced by UV irradiation *(39,40).* Fig. 3, D, shows that this inhibitory tyrosine phosphorylation of Cdk4 was present in serum-starved HCT116 cells. We then asked if CINK4 would prevent dephosphorylation of Cdk4 when these cells were transferred to serum-containing medium to induce them to re-enter the cell cycle. Fig. 3, D, shows that CINK4 treatment maintained the tyrosine phosphorylation on Cdk4 on restimulation of serum-starved HCT116 cells, whereas cells restimulated in the absence of CINK4 lost the tyrosine phosphorylation and re-entered the cell cycle. Roscovitine, by contrast, which inhibits Cdk2 at a later time in G_1 but not Cdk4 *(41),* failed to maintain tyrosine phosphorylation of Cdk4 on restimulation of serum-starved HCT116 cells (Fig. 3, D). This result strongly suggests that CINK4 acts by inhibiting Cdk4.

Effects of CINK4 on S-Phase Progression

We predicted that, if CINK4 was a specific inhibitor of Cdk4 activity, treated cells would not be affected once they had entered late G_1 phase and had passed the point in the cell cycle at which Cdk4 activity is required. To test this hypothesis, we treated U2OS cells with mimosine, a nonprotein amino acid from plants that inhibits eukaryotic DNA polymerase α, to block them at the G_1/S boundary *(42)* and then released the cells from the mimosine block by placing them in fresh medium that lacked mimosine and either contained or lacked CINK4. We then determined the cell cycle profiles at 16 and 38 hours after mimosine was removed from the cells and found that neither 5 nor 10 μ*M* CINK4 prevented the cells from proceeding further in the cell cycle (Table 2). Cells released in the presence of 5 μ*M* CINK4 completed the cell cycle and then arrested at the following G_1 phase. However, cells released from the mimosine block in the presence of 10 μ*M* CINK4 completed the cell cycle and then died at the following G_1 phase (Table 2). In contrast, mimosine-blocked cells placed in fresh medium lacking mimosine and containing the Cdk2-specific inhibitor roscovitine, which blocks cells at the G_1/S boundary, did not re-enter the cell cycle (data not shown). These results suggest that CINK4 has little effect on cell cycle progression once cells have entered the late G_1 phase and have proceeded beyond the point in the cell cycle at which Cdk4 activity is required. Therefore, they further confirm the specificity of CINK4 as a Cdk4 inhibitor.

Table 2. Cell cycle analysis of mimosine-treated U2OS osteosarcoma cells*

Treatment	% Cells in different phases of the cell cycle, %			
	G_0/G_1	S	G_2/M	SubG_1
Control	53.4	33.6	12.0	1
Mimosine (32 h)	73.7	21.0	4.5	0.8
Released (16 h)	17.2	33.0	47.6	2.2
Released, 5 μ*M* CINK4 (16 h)	16.7	29.5	41.0	12.8
Released, 10 μ*M* CINK4 (16 h)	20.7	39.2	18.3	21.8
Released (38 h)	39.6	23.1	32.3	5
Released, 5 μ*M* CINK4 (38 h)	34.8	20.6	31.4	13.2
Released, 10 μ*M* CINK4 (38 h)	14.3	15.8	13.9	56

*Cells were untreated (control) or treated with mimosine for 32 hours in 10% serum-containing medium and released in the presence of 10% serum with and without 5 and 10 μ*M* CINK4 (a chemical inhibitor of cyclin-dependent kinase 4) for 16 and 38 hours. Flow cytometry was used to determine the percentage of cells with a sub-G_1 DNA content and those in the G_0G_1, S, and G_2/M phases of the cell cycle.

Effect of CINK4 on Induction of Senescence-Associated Markers

Cdk4 inhibition by the Cdk4-specific inhibitory protein, p16, induces senescence *(43–46).* Senescence resembles G_0, a state that is analogous to terminal differentiation. The induction of senescence-associated markers, such as senescence-associated β-galactosidase (SA β-gal), in various cancer and normal cells by p16 thus involves inhibition of Cdk4. To determine if CINK4 mimics p16 in its ability to induce senescence, we asked if SA β-gal expression was induced in cells that lack functional p16 when they are treated with CINK4. U2OS cells treated with 5 and 10 μ*M* CINK4 for 24 and 48 hours were stained to detect SA β-gal activity *(44).* Approximately 25% of the cells treated with 5 μ*M* CINK4 were strongly positive for SA β-gal activity, while 10% of the cells were weakly stained (data not shown). In contrast, approximately 5% of the cells treated with 10 μ*M* CINK4 for 24 hours expressed SA β-gal activity, while longer treatment resulted in considerable cell death. From these results, we conclude that, like p16, Cdk4 inhibition by CINK4 can lead to senescence or apoptosis, depending on the concentration of the inhibitor.

Effects of Prolonged Treatment of Cells With 10 μ*M* CINK4

Prolonged treatment of U2OS cells with CINK4 resulted in considerable cell death. To determine if the U2OS cells were dying by apoptosis, we treated them with 5 and 10 μ*M* CINK4 for 48 hours and then subjected them to TUNEL analysis to detect the DNA strand breaks that characterize apoptotic cell death. Fig. 4 shows that a 48-hour treatment of U2OS cells with 5 μ*M* CINK4 had little effect on the induction of apoptosis, whereas a 48-hour treatment with 10 μ*M* CINK4 resulted in apoptosis in 83% of the cells. These results were qualitatively confirmed by use of a second assay for apoptosis that detects DNA fragmentation (data not shown). The majority of the apoptotic cells were blocked in G_1. Similar results were obtained by treating HCT116 cells for extended times with 10 μ*M* CINK4 (data not shown). Our results suggest that a delicate balance exists between senescence and apoptosis in U2OS and HCT116 cells that are treated with CINK4: Treatment at lower concentrations and for shorter times with this Cdk4 inhibitor causes

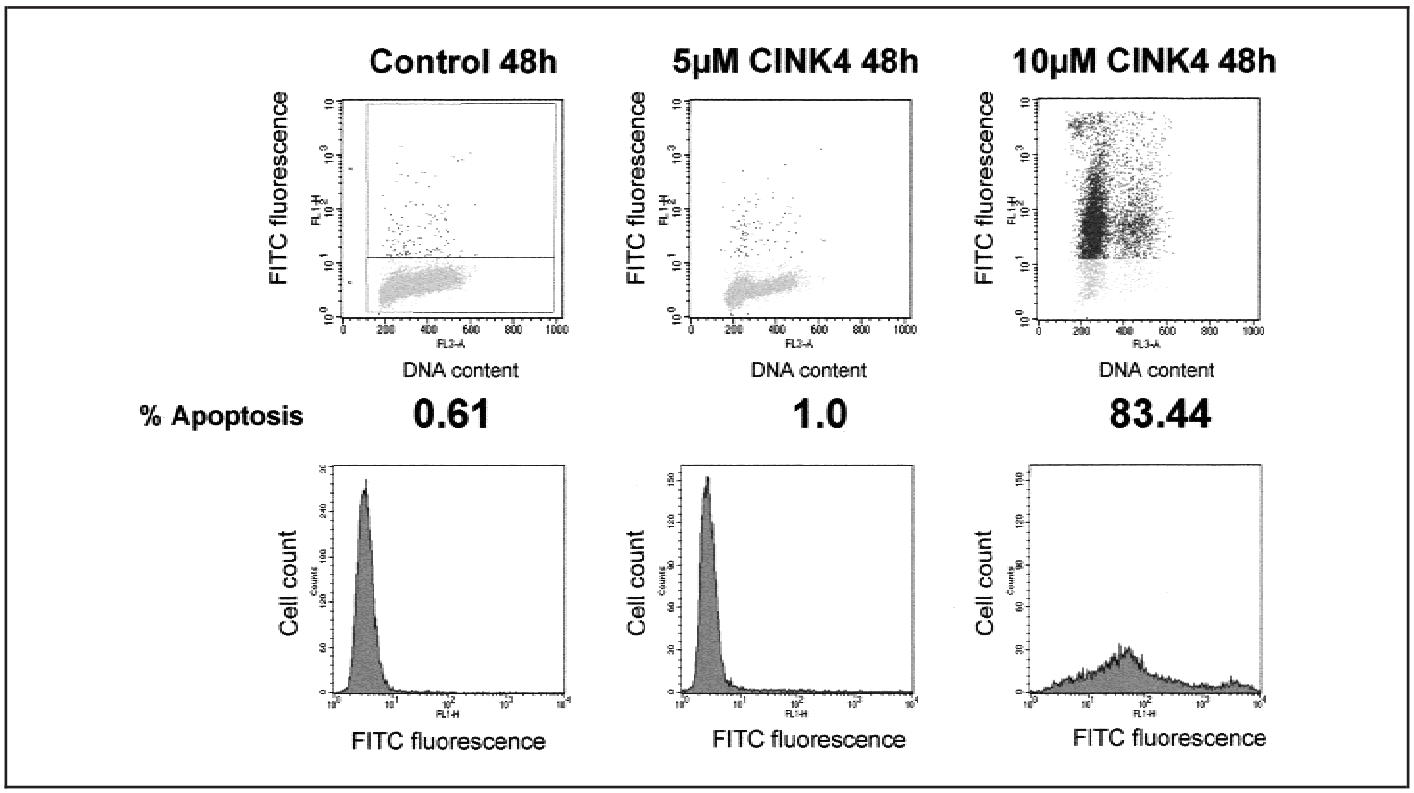

Fig. 4. Induction of apoptosis on prolonged treatment of U2OS cells with 10 μ*M* CINK4 (a chemical inhibitor of cyclin-dependent kinase 4) (48 hours). The **top row** shows fluorescence intensity of a fluorescein isothiocyanate (FITC)-labeled antibody to terminal deoxynucleotidyl transferase-mediated bromodeoxyuridine, which is a measure of DNA fragmentation, plotted as a function of total DNA content. An intensity of less than 10^1 corresponds to cells with intact DNA, while an intensity of greater than 10^1 corresponds to cells with fragmented DNA (apoptotic cells). The **bottom row** shows the number of cells plotted as a function of FITC fluorescence intensity (a measure of fragmented DNA). A shift of the peak to higher fluorescence intensity corresponds to an increase in DNA fragmentation.

cells to initiate senescence, whereas prolonged treatment at higher concentrations drives cells into apoptosis. Of interest, p16, a natural Cdk4 inhibitor, behaves similarly in that it induces senescence in some cases and apoptosis in others. This behavior may be due to different levels of p16 being expressed in different cellular contexts *(47).*

Effect of pRb on CINK4 Inhibition of Cdk4

The natural Cdk4 inhibitor, p16, mediates its growth-inhibitory function via pRb. We, therefore, tested if CINK4 inhibition of Cdk4 was also dependent on functional pRb. For these studies, we used two pairs of cell lines that differed from each other in the means by which pRb was functionally inactivated. The first pair of cell lines consisted of mouse NIH3T3 cells *(48),* which have functional pRb (pRb positive), and a congenic cell line that contains a homozygous deletion of pRb (pRb negative); the second pair consisted of U2OS cells and U2OS-TAg, a U2OS-derived cell line that was stably transformed with simian virus 40 large T antigen *(49),* which functionally inactivates pRb. Thus, U2OS cells are pRb positive and p16 negative, while U2OS-TAg cells are pRb negative and p16 negative. CINK4 treatment caused a cell cycle block in NIH3T3 pRb-positive cells, while the congenic pRb-negative cells were unaffected (Table 3). Similarly, U2OS cells (pRb positive) arrested in G_1 on treatment with CINK4, while the U2OS-TAg cells (pRb negative) did not. These results suggest that Cdk4 inhibition by CINK4 requires the presence of functional pRb.

Table 3. Functional retinoblastoma protein (pRb) is required for CINK4 (chemical inhibitor of cyclin-dependent kinase 4)-mediated growth arrest*

Cells	Treatment†	pRb status‡	% of cells in G_0/G_1	% of cells in S	G_0/G_1 : S ratio§
NIH3T3‖	Control	+	44.7	12.2	3.7
		–	43.5	20.0	2.2
	5 μ*M* CINK4	+	92.3	3.2	29.0
		–	49.8	9.1	5.5
	10 μ*M* CINK4	+	88.4	3.1	28.3
		–	48.7	11.6	4.2
U2OS¶	Control	+	49.8	19.9	2.5
		–	42.5	30.3	1.4
	5 μ*M* CINK4	+	79.5	11.0	7.2
		–	44.8	26.3	1.7
	10 μ*M* CINK4	+	82.9	3.6	23.1
		–	42.8	25.1	1.7

*Cell cycle analyses of NIH3T3 mouse fibroblast cells and U2OS human osteosarcoma cells as determined by flow cytometry.

†Control = untreated cells; 5 and 10 μ*M* CINK4 treatments were for 24 hours.

‡+ = cells express functional pRb; – = cells do not express functional pRb.

§The G_0/G_1 : S ratio is a measure of the percentage of cells blocked in G_1.

‖NIH3T3 cells normally express both p16 and pRb ($p16^{positive}$ and $pRb^{positive}$). A congenic cell line that contains a homozygous deletion of the retinoblastoma gene and, therefore, lacks functional pRb ($p16^{positive}$ and $pRb^{negative}$) was used to test the effect of pRb on CINK4-mediated growth arrest.

¶U2OS cells lack p16 but normally express pRb ($p16^{negative}$ and $pRb^{positive}$). U2OS-TAg, a U2OS-derived cell line that was stably transformed with simian virus 40 large T antigen *(49),* which functionally inactivates pRb ($p16^{negative}$ and $pRb^{negative}$), was used to test the effect of pRb on CINK4-mediated growth arrest.

This again indicates that, like p16, CINK4 requires pRb to manifest its action.

Effect of CINK4 on Established Tumors

We tested the efficacy of CINK4 as a Cdk4 inhibitor in a mouse xenograft model by using tumors derived from human HCT116 colon carcinoma cells. Initial pharmacokinetic experiments indicated that administration of CINK4 at 30 mg/kg intraperitoneally every 12 hours was sufficient to maintain the concentration of CINK4 in the tumors greater than 0.5 μM, a concentration that was necessary to inhibit the growth of those cells *in vitro* by 50% (data not shown). CINK4 treatment was initiated 20 days after the subcutaneous injection of HCT116 cells into nude mice, when the tumors had a volume of approximately 100 mm^3, and was continued for 29 days.

Fig. 5 shows that, after 29 days of treatment, CINK4 resulted in a statistically significant ($P = .031$) smaller final tumor volume (586 mm^3; 95% confidence interval [CI] = 383 to 789 mm^3) compared with tumors in mice treated with vehicle control (1088 mm^3; 95% CI = 611 to 1565 mm^3). However, mice treated for the same length of time with 5-fluorouracil had an even greater reduction in final tumor volume (to 327 mm^3; 95% CI = 175 to 479 mm^3). Although CINK4 treatment slowed tumor growth rates by approximately 17% compared with treatment with vehicle control, this reduction in growth rate failed to reach statistical significance by the Dunnett test ($P = .1$) but was statistically significant as determined by the less conservative Student's *t*–Newman–Keuls tests ($P = .028$). 5-Fluorouracil had a more dramatic effect, showing an approximately 60% reduction in tumor growth rate compared with controls or CINK4 ($P<.001$ for both) (Fig. 5, inset). The mice appeared to tolerate both the CINK4 and the 5-fluorouracil treatments, despite experiencing an approximately 20% reduction in body weight during the course of those treatments. A second independent experiment, which resulted in mean final tumor volumes of 960 mm^3 (95% CI = 639 to 1281 mm^3) for controls, 598 mm^3 (95% CI = 343 to 853 mm^3) for CINK4 treatment, and 280 mm^3 (95% CI = 203 to 357 mm^3) for 5-fluorouracil treatment, confirmed the *in vivo* antitumor activity of CINK4 against HCT116-derived tumors ($P = .035$ for both treatment groups versus controls as analyzed by the Dunnett test). Thus, CINK4 treatment was effective *in vivo* in inhibiting the growth of tumors derived from cells that lack p16 but possess functional pRb.

Discussion

We show here that CINK4, a triaminopyrimidine derivative, specifically inhibits Cdk4 in an *in vitro* kinase assay and reduces tumor volume in a mouse model. Cdk4 is the key kinase that, by phosphorylating pRb, is required for cell cycle entry and for cells to emerge from quiescence *(40,50).* It should be noted that, in some systems, the activities of Cdk4 and Cdk6 may be responsible for only a component of the phosphorylation of pRb and that hyperphosphorylation of pRb, which is necessary for its growth-inhibitory effects, requires subsequent phosphorylations by Cdk2 *(51).* However, initial phosphorylation by Cdk4 and Cdk6 may nevertheless be required for later Cdk2-mediated actions.

Most human tumors have alterations in the p16/Cdk4/pRb pathway. Tumors deficient in p16 grow unabatedly, presumably because Cdk4 is constitutively active in the absence of its natural inhibitor. Therefore, inhibiting Cdk4 activity in tumors that lack

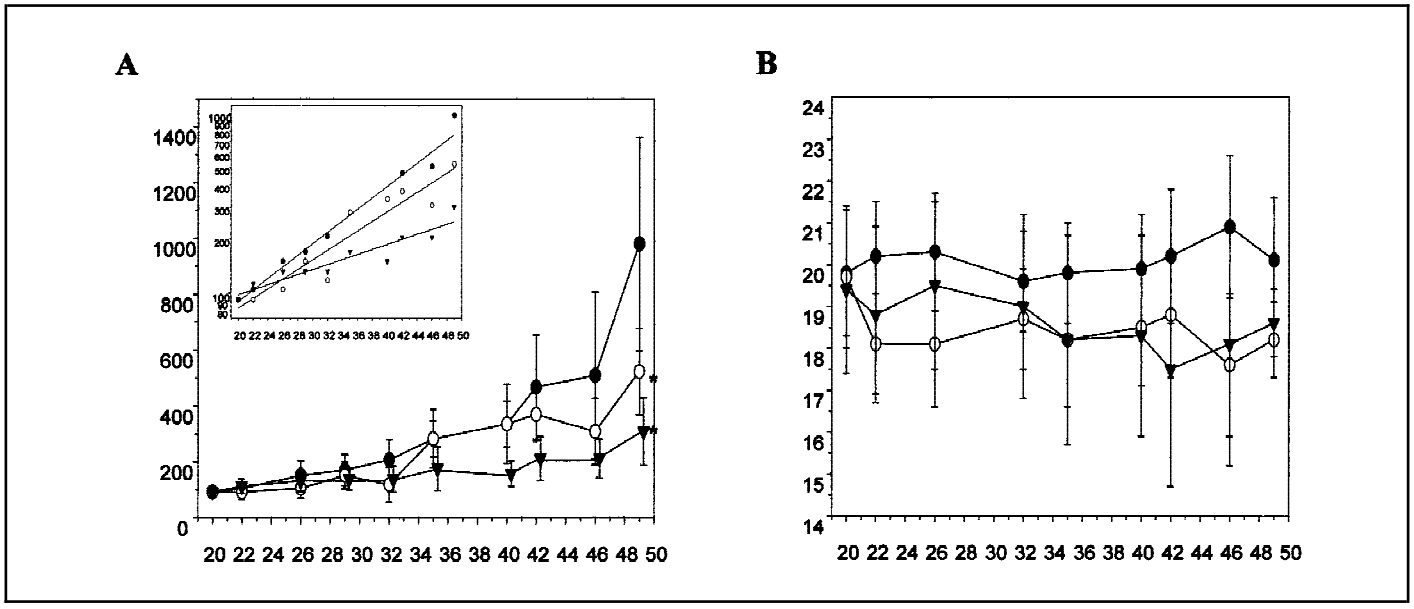

Fig. 5. Effect of CINK4 (a chemical inhibitor of cyclin-dependent kinase 4) on the volume of xenograft tumors derived from HCT116 human colon carcinoma cells. Mice bearing tumors derived from the injection of HCT116 cells were treated with vehicle controls (5% dimethyl sulfoxide/0.05% Tween 80/95% physiologic saline), 5-fluorouracil (75 mg/kg, once per week, by intravenous injection), or CINK4 (30 mg/kg, every 12 hours, by intraperitoneal injection) starting on day 21 after injection of HCT116 cells. **Panel A:** tumor volumes over time. The ***y*-axis** shows tumor volumes (in median mm^3), and the ***x*-axis** shows the number of days after HCT116 cells were injected into the mice. The **inset** shows the tumor volume data plotted on a logarithmic scale. The growth rates (**slopes**) of tumors from control mice (0.0346 ± 0.00219 SEM) were greater than those of tumors from CINK4-treated (0.0287 ± 0.00106 SEM; $P = .028$) or 5-fluorouracil-treated (0.0138 ± 0.00182 SEM; $P<.001$) mice (by use of the Student's *t*–Newman–Keuls tests). **Panel B:** body weights over time. The ***y* axis** shows body weights (in mean grams), and the ***x*-axis** shows the number of days after HCT116 cells were injected into the mice. In both graphs, the **filled circles** represent mice treated with vehicle controls, the **unfilled circles** represent treatment with CINK4, and the **filled inverted triangles** represent 5-fluorouracil treatment. **Bars** = 95% confidence intervals. SEM = standard error of the mean.

p16 is essential to stop cell proliferation. CINK4 meets this criterion: It replaces the activity of p16 in cells that lack p16 by inhibiting Cdk4, most likely through direct binding to the ATP-binding pocket of the kinase. Consistent with its *in vitro* inhibition of Cdk4, CINK4 arrested the growth of asynchronous MRC-5 and U2OS cells with concomitant loss of Ser780 and Ser795 phosphorylations in the endogenous Cdk4 substrate, pRb. However, normal diploid fibroblast MRC-5 cells resumed the cell cycle after CINK4 was removed, while U2OS cells treated in a similar fashion underwent appreciable cell death (data not shown). CINK4 prevented cell cycle re-entry not only of serum-starved MRC-5 and HCT116 cells but also of U2OS cells after release from quinidine block, further suggesting inhibition of Cdk4 by CINK4. CINK4, however, had little effect on progression through S phase (Table 2). Moreover, Cdk4 immunoprecipitated from CINK4-treated HCT116 cells had statistically significantly less kinase activity than did Cdk4 immunoprecipitated from untreated cells, presumably because the activity of the kinase in the treated cells was inhibited by CINK4. These biochemical observations indicate that CINK4 prevents Cdk4 from phosphorylating pRb, thereby abolishing entry of quiescent G_0 cells into the cell cycle. Although p16 and its derived peptides have been shown to behave similarly to each other *(52–57),* the precise physiologic role of p16 remains unclear. Nevertheless, our results with CINK4, which mostly parallel those that have been published with p16, suggest that CINK4-mediated prevention of pRb phosphorylation and inhibition of cell growth are a consequence of Cdk4 inhibition *(52–57).*

It has been reported that cellular accumulation of p16 induces senescence *(43–45,58).* Of interest, treatment of cells with 5 μ*M* CINK4 also induced expression of a senescence-associated marker, SA β-gal, suggesting that induction of senescence in both cases could be due to the inhibition of Cdk4. However, senescence was "bypassed" when cells either were treated with a higher concentration of CINK4 (10 μ*M*) or were exposed for a prolonged period (48 hours) to 5 μ*M* CINK4, both of which caused cells to undergo apoptosis. Ectopic expression of the endogenous Cdk4 inhibitor p16 produces similar results *(45,47).* These observations suggest that the phenomena of senescence and apoptosis may be linked and that the extent of Cdk4 inhibition may determine whether cells enter into senescence or apoptosis. This possibility warrants further research to identify gene(s) that are deregulated by Cdk4 inhibition *per se* and that play a role in senescence and/or apoptosis.

A plethora of synthetic Cdk inhibitors have been described in the literature *(28,59–62)* that inhibit either both Cdk2 and Cdk4 or all Cdks nonspecifically. A model for a synthetic tumor suppressor molecule based on the cyclin-dependent kinase inhibitory domain of the INK4 family has also been described, suggesting the importance of Cdk4 inhibition in blocking tumor growth *(63).* It was reported recently that certain diaminothiazole derivatives could act as selective inhibitors of Cdk4 *(64).* CINK4 is among this emerging class of small molecule inhibitors that are unique in their selectivity for Cdk4. Our demonstration that CINK4 drastically reduces tumor volume in an *in vivo* mouse model suggests that CINK4 or compounds with similar structures could have important clinical value for treating tumors that either lack p16 (e.g., non-small-cell lung carcinomas) or contain deregulated Cdk4 activity [e.g., hepatoblastomas *(65)*]. Our results also suggest that CINK4 could be useful for studying aspects of cell growth and differentiation linked to senescence and apoptosis, especially in cells lacking p16 but possessing functional pRb.

REFERENCES

(1) Pines J. Four-dimensional control of the cell cycle. Nat Cell Biol 1999;1: E73–9.

(2) Yang J, Kornbluth S. All aboard the cyclin train: subcellular trafficking of cyclins and their CDK partners. Trends Cell Biol 1999;9:207–10.

(3) Pavletich NP. Mechanisms of cyclin-dependent kinase regulation: structures of Cdks, their cyclin activators, and Cip and INK4 inhibitors. J Mol Biol 1999;287:821–8.

(4) Morgan DO. Cyclin-dependent kinases: engines, clocks, and microprocessors. Annu Rev Cell Dev Biol 1997;13:261–91.

(5) Sherr CJ. Cancer cell cycles. Science 1996;274:1672–7.

(6) Sherr CJ, Roberts JM. Inhibitors of mammalian G1 cyclin-dependent kinases. Genes Dev 1995;9:1149–63.

(7) Bartek J, Bartkova J, Lukas J. The retinoblastoma protein pathway and the restriction point. Curr Opin Cell Biol 1996;8:805–14.

(8) Lundberg AS, Weinberg RA. Functional inactivation of the retinoblastoma protein requires sequential modification by at least two distinct cyclin-cdk complexes. Mol Cell Biol 1998;18:753–61.

(9) Weinberg RA. The retinoblastoma protein and cell cycle control. Cell 1995;81:323–30.

(10) Dyson N. The regulation of E2F by pRB-family proteins. Genes Dev 1998; 12:2245–62.

(11) Lukas J, Parry D, Aagaard L, Mann DJ, Bartkova J, Strauss M, et al. Retinoblastoma-protein-dependent cell-cycle inhibition by the tumour suppressor p16. Nature 1995;375:503–6.

(12) Shapiro GI, Rollins BJ. p16INK4A as a human tumor suppressor. Biochim Biophys Acta 1996;1242:165–9.

(13) Palmero I, Peters G. Perturbation of cell cycle regulators in human cancer. Cancer Surv 1996;27:351–67.

(14) Okamoto A, Demetrick DJ, Spillare EA, Hagiwara K, Hussain SP, Bennett WP, et al. Mutations and altered expression of p16INK4A in human cancer. Proc Natl Acad Sci USA 1994;91:11045–9.

(15) Medema RH, Herrera RE, Lam F, Weinberg RA. Growth suppression by p16INK4A requires functional retinoblastoma protein. Proc Natl Acad Sci USA 1995;92:6289–93.

(16) Guan KL, Jenkins CW, Li Y, Nichols MA, Wu X, O'Keefe CL, et al. Growth suppression by p18, a p16 INK4/MTS1- and p14 INK4/MTS2-related CDK6 inhibitor, correlates with wild-type pRb function. Genes Dev 1994;8:2939–52.

(17) Shapiro GI, Park JE, Edwards CD, Mao L, Merlo A, Sidransky D, et al. Multiple mechanisms of p16INK4A inactivation in non-small cell lung cancer cell lines. Cancer Res 1995;55:6200–9.

(18) Sakaguchi M, Fujii Y, Hirabayashi H, Yoon HE, Komoto Y, Oue T, et al. Inversely correlated expression of p16 and Rb protein in non-small cell lung cancers: an immunohistochemical study. Int J Cancer 1996;65:442–5.

(19) Shapiro GI, Edwards CD, Kobzik L, Godleski J, Richards W, Sugarbaker DJ, et al. Reciprocal Rb inactivation and p16INK4A expression in primary lung cancers and cell lines. Cancer Res 1995;55:505–9.

(20) Wu JJ, Yarwood DR, Sills MA, Chaudhuri B, Muller L, Zurini M. Measurement of cdk4 kinase activity using an affinity peptide-tagging technology. Comb Chem High Throughput Screen 2000;3:27–36.

(21) Kato JY, Matsuoka M, Strom DK, Sherr CJ. Regulation of cyclin D-dependent kinase 4 (cdk4) by cdk4-activating kinase. Mol Cell Biol 1994; 14:2713–21.

(22) Kato J, Matsushime H, Hiebert SW, Ewen ME, Sherr CJ. Direct binding of cyclin D to the retinoblastoma gene product (pRb) and pRb phosphorylation by the cyclin D-dependent kinase CDK4. Genes Dev 1993;7:331–42.

(23) Kitagawa M, Higashi H, Jung HK, Suzuki-Takahashi I, Ikeda M, Tamai K, et al. The consensus motif for phosphorylation by cyclin D1-Cdk4 is different from that for phosphorylation by cyclin A/E-Cdk2. EMBO J 1996; 15:7060–9.

(24) Moorthamer M, Zumstein-Mecker S, Chaudhuri B. DNA binding protein dbpA binds Cdk5 and inhibits its activity. FEBS Lett 1999;446:343–50.

(25) Matsushime H, Quelle DE, Shurtleff SA, Shibuya M, Sherr CJ, Kato JY. D-type cyclin-dependent kinase activity in mammalian cells. Mol Cell Biol 1994;14:2066–76.

(26) Harper JW, Elledge SJ, Keyomarsi K, Dynlacht B, Tsai LH, Zhang P, et al. Inhibition of cyclin-dependent kinases by p21. Mol Biol Cell 1995;6: 387–400.
(27) Phelps DE, Xiong Y. Assay for activity of mammalian cyclin D-dependent kinases CDK4 and CDK6. Methods Enzymol 1997;283:194–205.
(28) Mohamadi F, Richards NG, Guida WC, Liskamp R, Lipton M, Caufield C, et al. Macromodel—an integrated software system for modeling organic and bioorganic molecules using molecular mechanics. J Comp Chem 1990; 11:440–67.
(29) Schulze-Gahmen U, Brandsen J, Jones HD, Morgan DO, Meijer L, Vesely J, et al. Multiple modes of ligand recognition: crystal structures of cyclin-dependent protein kinase 2 in complex with ATP and two inhibitors, olomoucine and isopentenyladenine. Proteins 1995;22:378–91.
(30) Hanks SK, Quinn AM. Protein kinase catalytic domain sequence database: identification of conserved features of primary structure and classification of family members. Methods Enzymol 1991;200:38–62.
(31) Bostrom J, Norrby PO, Liljefors T. Conformational energy penalties of protein-bound ligands. J Comput Aided Mol Des 1998;12:383–96.
(32) Bernardi A, Raimondi L, Zuccotto F. Simulation of protein–sugar interactions: a computational model of the complex between ganglioside GM1 and the heat-labile enterotoxin of *Escherichia coli.* J Med Chem 1997;40: 1855–62.
(33) Senderowicz AM. Flavopiridol: the first cyclin-dependent kinase inhibitor in human clinical trials. Invest New Drugs 1999;17:313–20.
(34) Fabbro D, Buchdunger E, Wood J, Mestan J, Hofmann F, Ferrari S, et al. Inhibitors of protein kinases: CGP 41251, a protein kinase inhibitor with potential as an anticancer agent. Pharmacol Ther 1999;82:293–301.
(35) Jeffrey PD, Russo AA, Polyak K, Gibbs E, Hurwitz J, Massague J, et al. Mechanism of CDK activation revealed by the structure of a cyclin A–CDK2 complex. Nature 1995;376:313–20.
(36) Grafstrom RH, Pan W, Hoess RH. Defining the substrate specificity of cdk4 kinase–cylcin D1 complex. Carcinogenesis 1999;20:193–8.
(37) Connell-Crowley L, Harper JW, Goodrich DW Cyclin D1/Cdk4 regulates retinoblastoma protein-mediated cell cycle arrest by site-specific phosphorylation. Mol Biol Cell 1997;8:287–301.
(38) Wang S, Melkoumian Z, Woodfork KA, Cather C, Davidson AG, Wonderlin WF, et al. Evidence for an early G1 ionic event necessary for cell cycle progression and survival in the MCF-7 human breast carcinoma cell line. J Cell Physiol 1998;176:456–64.
(39) Terada Y, Tatsuka M, Jinno S, Okayama H. Requirement for tyrosine phosphorylation of Cdk4 in G1 arrest induced by ultraviolet irradiation. Nature 1995;376:358–62.
(40) Jinno S, Hung SC, Okayama H. Cell cycle start from quiescence controlled by tyrosine phosphorylation of Cdk4. Oncogene 1999;18:565–71.
(41) Schutte B, Nieland L, van Engeland M, Henfling ME, Meijer L Ramaekers FC. The effect of the cyclin-dependent kinase inhibitor olomoucine on cell cycle kinetics. Exp Cell Res 1997;236:4–15.
(42) Ji C, Marnett LJ, Pietenpol JA. Cell cycle re-entry following chemically-induced cell cycle synchronization leads to elevated p53 and p21 protein levels. Oncogene 1997;15:2749–53.
(43) Taniguchi K, Kohsaka H, Inoue N, Terada Y, Ito H, Hirokawa K, et al. Induction of the p16INK4a senescence gene as a new therapeutic strategy for the treatment of rheumatoid arthritis. Nat Med 1999;5:760–7.
(44) Serrano M, Lin AW, McCurrach ME, Beach D, Lowe SW. Oncogenic ras provokes premature cell senescence associated with accumulation of p53 and p16INK4a. Cell 1997;88:593–602.
(45) McConnell BB, Starborg M, Brookes S, Peters G. Inhibitors of cyclin-dependent kinases induce features of replicative senescence in early passage human diploid fibroblasts. Curr Biol 1998;8:351–4.
(46) Dimri GP, Lee X, Basile G, Acosta M, Scott G, Roskelley C, et al. A biomarker that identifies senescent human cells in culture and in aging skin *in vivo.* Proc Natl Acad Sci USA 1995;92:9363–7.
(47) Naruse I, Heike Y, Hama S, Mori M, Saijo N. High concentrations of recombinant adenovirus expressing p16 gene induces apoptosis in lung cancer cell lines. Anticancer Res 1998;18:4275–82.
(48) Peeper DS, Upton TM, Ladha MH, Neuman E, Zalvide J, Bernards R, et al. Ras signalling linked to the cell-cycle machinery by the retinoblastoma protein. Nature 1997;386:177–81.
(49) Wang JY, Knudsen ES, Welch PJ. The retinoblastoma tumor suppressor protein. Adv Cancer Res 1994;64:25–85.
(50) Ladha MH, Lee KY, Upton TM, Reed MF, Ewen ME. Regulation of exit from quiescence by p27 and cyclin D1-CDK4. Mol Cell Biol 1998;18: 6605–15.
(51) Harbour JW, Luo RX, Dei Santi A, Postigo AA, Dean DC. Cdk phosphorylation triggers sequential intramolecular interactions that progressively block Rb functions as cells move through G1. Cell 1999;98:859–69.
(52) Byeon IJ, Li J, Ericson K, Selby TL, Tevelev A, Kim HJ, et al. Tumor suppressor p16INK4A: determination of solution structure and analyses of its interaction with cyclin-dependent kinase 4. Mol Cell 1998;1:421–31.
(53) Fahraeus R, Paramio JM, Ball KL, Lain S, Lane DP. Inhibition of pRb phosphorylation and cell-cycle progression by a 20-residue peptide derived from p16CDKN2/INK4A. Curr Biol 1996;6:84–91.
(54) Lee KY, Yoo CG, Han SK, Shim YS, Kim YW. The effects of transferring tumor suppressor gene p16INK4A to p16INK4A-deleted cancer cells. Korean J Intern Med 1999;14:53–8.
(55) Lee JH, Lee CT, Yoo CG, Hong YK, Kim CM, Han SK, et al. The inhibitory effect of adenovirus-mediated p16INK4a gene transfer on the proliferation of lung cancer cell line. Anticancer Res 1998;18:3257–61.
(56) Gius DR, Ezhevsky SA, Becker-Hapak M, Nagahara H, Wei MC, Dowdy SF. Transduced p16INK4a peptides inhibit hypophosphorylation of the retinoblastoma protein and cell cycle progression prior to activation of Cdk2 complexes in late G1. Cancer Res 1999;59:2577–80.
(57) Frost SJ, Simpson DJ, Clayton RN, Farrell WE. Transfection of an inducible p16/CDKN2A construct mediates reversible growth inhibition and G1 arrest in the AtT20 pituitary tumor cell line. Mol Endocrinol 1999;13: 1801–10.
(58) Hara E, Smith R, Parry D, Tahara H, Stone S, Peters G. Regulation of p16CDKN2 expression and its implications for cell immortalization and senescence. Mol Cell Biol 1996;16:859–67.
(59) Havlicek L, Hanus J, Vesely J, Leclerc S, Meijer L, Shaw G, et al. Cytokinin-derived cyclin-dependent kinase inhibitors: synthesis and cdc2 inhibitory activity of olomoucine and related compounds. J Med Chem 1997; 40:408–12.
(60) Zaharevitz DW, Gussio R, Leost M, Senderowicz AM, Lahusen T, Kunick C, et al. Discovery and initial characterization of the paullones, a novel class of small-molecule inhibitors of cyclin-dependent kinases. Cancer Res 1999;59:2566–9.
(61) Hoessel R, Leclerc S, Endicott JA, Nobel ME, Lawrie A, Tunnah P, et al. Indirubin, the active constituent of a Chinese antileukaemia medicine, inhibits cyclin-dependent kinases. Nat Cell Biol 1999;1:60–7.
(62) Kent LL, Hull-Campbell NE, Lau T, Wu JC, Thompson SA, Nori M. Characterization of novel inhibitors of cyclin-dependent kinases. Biochem Biophys Res Commun 1999;260:768–74.
(63) Fahraeus R, Lain S, Ball KL, Lane DP. Characterization of the cyclin-dependent kinase inhibitory domain of the INK4 family as a model for a synthetic tumour suppressor molecule. Oncogene 1998;16:587–96.
(64) Lundgren K, Price SM, Escobar J, Huber A, Chong W, Li L, et al. Diaminothiazoles: potent selective cyclin-dependent kinase inhibitors with antitumor efficacy [abstract]. Clin Cancer Res Suppl 1999;5:3755s.
(65) Kim H, Ham EK, Kim YI, Chi JG, Lee HS, Park SH, et al. Overexpression of cyclin D1 and cdk4 in tumorigenesis of sporadic hepatoblastomas. Cancer Lett 1998;131:177–83.
(66) Schriever C, Breithardt G, Schmidt A. Undersulfation of proteoheparan sulfate stimulates the expression of basic fibroblast growth factor and protein synthesis but suppresses replication of coronary smooth muscle cells. Biol Chem 1997;378:701–6.

NOTES

Editor's note: T. O'Reilly, L. Muller, and C. Stephan own stock in Novartis Pharma AG.

Manuscript received May 24, 2000; revised January 4, 2001; accepted January 22, 2001.